

Effects of Non-Uniform Refrigerant and Air Flow Distributions on Finned-Tube Evaporator Performance

Jong Min Choi, W. Vance Payne and Piotr A. Domanski

National Institute of Standards and Technology
Building Environment Division
MS 8631, Building 226, Room B114
Gaithersburg, Maryland USA 20899
Phone: 301-975-6663 Fax: 301-975-8973 Email: vance.payne@nist.gov

ABSTRACT

An experimental investigation was implemented to determine the capacity degradation due to non-uniform refrigerant and air flow distributions, and to assess the potential to recover the lost capacity via controlling refrigerant distribution between individual refrigerant circuits. The tests were performed on a three-circuit, three-depth-row, finned-tube evaporator. Refrigerant inlet quality, exit saturation temperature, and exit superheats for the individual circuits were controlled.

The study showed that capacity degradation due to refrigerant maldistribution can be as much as 30 %, even when the overall evaporator superheat is kept at the target 5.6 °C. Experimental data indicate that part of this capacity degradation was caused by the internal heat transfer within the evaporator assembly. For the coil and air maldistributions studied, the maximum capacity degradation was found to be 8.7 %. A 4.0% capacity recovery was obtained by controlling refrigerant distribution to obtain the target 5.6 °C at each circuit exit.

INTRODUCTION

Most evaporators use an inlet expansion valve with a flow distributor to control the overall superheat at the evaporator exit manifold. In the evaporator, the refrigerant flows through parallel refrigerant circuits, which are designed to optimize between the benefit of improved refrigerant heat transfer and the penalty of refrigerant pressure drop. The coil performs optimally when the superheat at individual circuit exits matches the desired overall superheat in the exit manifold.

Evaporator air velocities may vary due to the geometry of the heat exchanger installation, nearness of the blower, blockage of the air filter, and other factors. Non-uniform air flow can cause some circuits to have excessive superheat while others may remain two-phase at the evaporator exit. In such situations, some circuits inefficiently use coil area when transferring heat with superheated vapor instead of two-phase refrigerant.

Liang et al. (2001) conducted a numerical study of an evaporator with various refrigerant circuits operating with uniform air flow. The researchers found that using a complex, optimized refrigerant circuit arrangement with refrigerant circuits properly branched may reduce the needed heat transfer area by about 5 % for the same capacity. Kirby et al. (1998) experimentally investigated the performance of a 5275 W window air conditioner under wet and dry coil conditions with non-uniform air flow over the evaporator. The velocity variation over the evaporator varied by a factor of 3, but upon correcting the non-uniformity of air flow, the investigators saw only a minor improvement in performance. Chwalowski et al. (1989) performed a simulation and experimental study of an evaporator operating with five different air velocities cause by different installations. In the extreme case, they reported a capacity difference of 30 %. Lee et al. (1997) executed a simulation study of an R22 and R407C evaporator with non-uniform air and refrigerant distributions. The study showed that the level of capacity degradation is affected by the refrigerant circuitry design and air velocity profile relative to that circuit. For the cases studied, they reported that the capacity of the evaporator showed a greater sensitivity to air maldistribution than to refrigerant maldistribution.

The goal of this study was to investigate the potential capacity improvements due to smart refrigerant distributors capable of controlling refrigerant distribution within each circuit. The experimental setup used a three-refrigerant-circuit evaporator with a system of valves, which allow controlling individual refrigerant superheats at the desired level. The effects of non-uniform refrigerant and air distributions were studied. A more detailed report of the this investigation is reported in Payne and Domanski (2003).

1. EXPERIMENTAL SETUP AND TEST PROCEDURE

1.1 Experimental Setup

Figure 1 shows a schematic of the experimental setup. The test rig consists of three major flow loops: (1) a refrigerant flow loop containing an evaporator, (2) a water flow loop used for the condenser, and (3) an air flow loop for the evaporator. The design of the rig allowed easy control of operating parameters such as condensing pressure and subcooling at the inlet of the expansion valve (evaporator inlet enthalpy), evaporating pressure and superheat at the exit of the evaporator.

An open-type reciprocating compressor with a variable speed motor was used to adjust the refrigerant mass flow rate. Condensing pressure and subcooling were set by changing the supplied water flow rate and temperature from the portable chiller to the condensing heat exchanger and subcooler, respectively. The control of condensing pressure and subcooling allows evaporator inlet quality to be controlled to within $\pm 1\%$.

Figure 2 presents the schematic of the R22 finned-tube evaporator used in this study. The evaporator has 54 smooth copper tubes placed in three depth rows and three parallel circuits. The tubes have louvered aluminum fins. Inlets of each circuit are connected to an individual manual expansion valve to adjust each circuit's exit superheat. A pressure-regulating valve controls the evaporator exit pressure. A Coriolis-type mass flow meter measures refrigerant flow rate in the liquid line between the subcooler and the expansion valves.

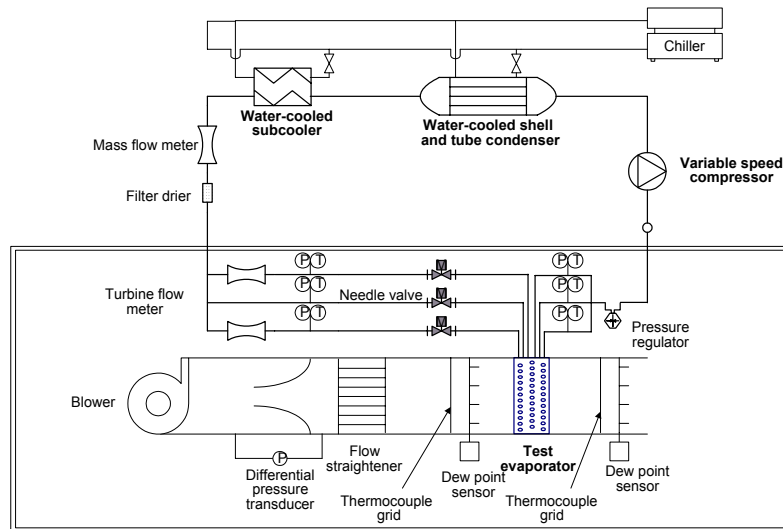


Figure 1: Experimental setup schematic

The test evaporator was installed in a multi-nozzle air flow chamber, which was constructed according to ANSI/AMCA 210 (1985). The exhaust fan installed at the exit of the air flow chamber controls air flow rate. All measurements and data reduction were in accordance with ASHRAE Standard 37 (1998). The maximum difference between the air and refrigerant side capacity was less than 5%.

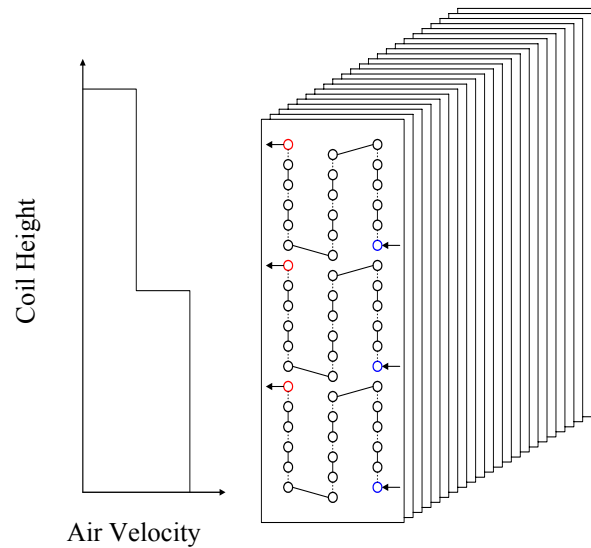


Figure 2: Evaporator circuiting with an example of non-uniform air velocity profile

1.2 Test Conditions and Procedure

The study included wet and dry-coil tests at 26.7 °C dry-bulb temperature. The dew-point temperature for wet-coil tests was 15.8 °C. R22 state at the inlet to the expansion valves was controlled to maintain an enthalpy equivalent to a 48.9 °C saturation temperature with a subcooling of 8.3 °C, which resulted in an evaporator inlet quality of 25 %. The evaporator exit was maintained at a pressure corresponding to saturation temperature of 7.2 °C. Indoor dry-bulb and dew-point were stabilized for at least one hour before test data were taken.

Table 1 presents the tests performed. Superheat conditions in the individual circuits were set by adjusting R22 mass flow through each circuit using three manual expansion valves. For tests with non-uniform air distribution, metal mesh plates were attached to the upper half of the coil to alter the velocity profile. Two kinds of non-uniform air flow tests were performed: 1) the volumetric air flow rate was held constant by increasing fan speed as the mesh blockage was added; 2) the volumetric air flow decreased as the mesh blockage was added.

A hot wire anemometer was used to measure the air flow rate by traversing the coil at a minimum of 25 equally spaced points at the face of the coil. This measurement agreed with the chamber air flow within 2 %.

Table 1: Test matrix

| Parameter | Air flow | Superheat at each circuit (°C) | | | | Test Name |
|------------------------------------------------------------|----------------------------------|--------------------------------|--------|--------|---------|-----------|
| | | Top | Middle | Bottom | Overall | |
| Imposed non-uniform refrigerant distribution | Uniform and constant | 5.6 | 5.6 | 5.6 | 5.6 | Case A |
| | | 16.7 | 16.7 | 16.7 | 16.7 | Case B |
| | | (1) | 16.7 | 16.7 | 5.6 | Case C |
| Imposed non-uniform air flow distribution by mesh blockage | Constant | (2) | (2) | (2) | (2) | Case D |
| | | 5.6 | 5.6 | 5.6 | 5.6 | Case E |
| | Reduced due to the mesh blockage | (2) | (2) | (2) | (2) | Case F |
| | | 5.6 | 5.6 | 5.6 | 5.6 | Case G |

(1) Expansion valve connected to top circuit was adjusted to set the overall superheat at 5.6 °C. (2) Superheat was not adjusted; the expansion valves remained unchanged from the superheat set at 5.6 °C with uniform air flow.

2. RESULTS AND DISCUSSION

2.1 Maldistributed Refrigerant Tests with Uniform Air Flow

Refrigerant may be improperly distributed between different circuits because of bends or other blockages in the distributor tubes, or because of non-optimal design. Figure 3 shows capacity variations at different imposed superheats scenarios for each circuit for dry and wet coil tests. Case A and Case B represent uniform superheat for all individual circuits of 5.6 °C and 16.7 °C, respectively. For Case C, the middle and bottom circuit superheats are 16.7 °C, while the top circuit is controlled to set an overall superheat of 5.6 °C. This required overfeeding of the top circuit, which resulted in its flooding.

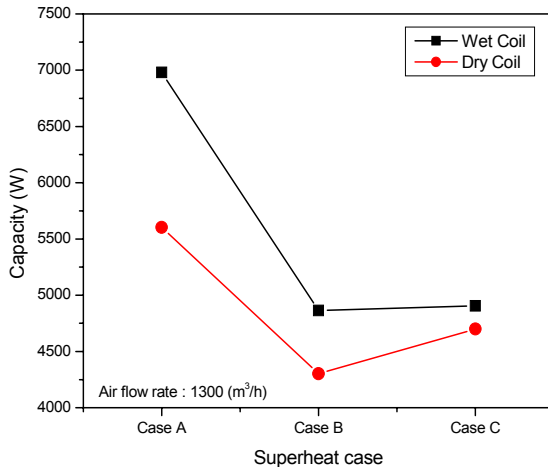


Figure 3: Capacity for different superheat control scenarios for dry- and wet-coil tests at uniform air flow

The tests show a rapid decrease in capacity when superheat increased in individual circuits. For Case B, the capacity drops by 32 % as the individual and overall superheats increased to 16.7 °C. It is interesting to note that a similar capacity degradation, 30 %, was measured for Case C, even though the overall superheat was held at 5.6 °C, and only two out of three circuits had superheated refrigerant. It appears that the existence of one flooded and two superheated circuits (and resulting significant temperature differences existing within the coil assembly) in Case C promoted internal heat transfer within the coil, which affected coil performance detrimentally.

To examine the effects of internal heat conduction via fins between different tube depth rows, a special coil was obtained from the manufacturer of the original coil. The original coil (Coil-E) and the special coil (Coil-EC) were identical except that the fins in Coil-EC were not continuous between tube depth rows but were cut to produce three separate tube banks. This arrangement prevented heat transfer via fins between tubes in different depth rows.

Figure 4 shows wet-coil tests results for Coil-E and Coil-EC for two air volumetric flow rates. For Case A, where all individual superheats were at 5.6 °C and no significant temperature differences existed in the coil assemblies, the capacity measured for both coils are very similar. (The slightly higher capacity measured for Coil-EC may be due to the additional tripping of the air boundary layer by the additional cuts in Coil-EC fins separating the tube depth rows.) For Case B, Coil-EC capacities were greater than Coil-E capacities by 10.2 % and 23.0 %, for 1300 m³/h and 1700 m³/h volumetric flow rates, respectively. In these tests, the superheat at all three circuits was controlled at 16.7 °C. The cuts made in Coil-EC fins separating different depth rows appeared to be the only plausible explanation for the Coil-EC higher capacity.

With the cross-counter flow of the refrigerant with respect to the air realized in the tested evaporator, superheated refrigerant existed in the most upstream tubes. This provided the opportunity for heat transfer between highly superheated refrigerant in the first-depth- row tubes with the two-phase refrigerant in the second depth row in Coil-E. This heat transfer was parasitic in nature because it did not directly aid in cooling the air.

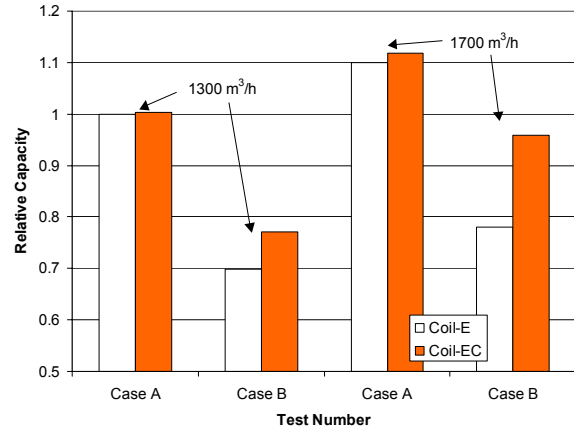


Figure 4: Capacity for a regular coil and a coil with separated depth rows for different superheat control scenarios referenced to the baseline capacity

2.2 Non-Uniform Air Flow Tests

Evaporator face velocity may vary due to air filter blockage, blower arrangement, heat exchanger geometry, etc. In this study, the combined effects of non-uniform air flow and evaporator superheat were examined by blocking the upper portion of the test evaporator. Baseline tests were first performed with 5.6 °C superheat for all circuits and uniform air velocity. Then, the blockage was applied and no expansion valve adjustment was made (case D or case F). Finally, the expansion valves were adjusted to yield 5.6 °C superheat on all circuits (case E or case G). Two series of tests, with a constant air flow and with the air flow decreased by the blockage were performed.

2.2.1. Constant Air Flow Rate: Tests with a constant air flow correspond to an installation scenario where the installer adjusted the fan speed to obtain the specified flow rate. Figure 5 shows capacity for different air velocity ratios, where velocity ratio is defined in this study as the ratio of the averaged air velocities between the top and bottom halves of the coil. Figure 6 presents capacity for different air velocity ratios referenced to the baseline capacity. For the velocity ratio of 1:1.26 and no superheat adjustment, the capacity decreased less than 1 %, and this capacity loss was recovered when superheat was corrected. For greater differences in air distributions, the capacity penalty was as much as 6 % (for the 2.59 velocity ratio), and when the superheat for each circuit was adjusted to 5.6 °C, the capacity recovered to within 2 % of the baseline value.

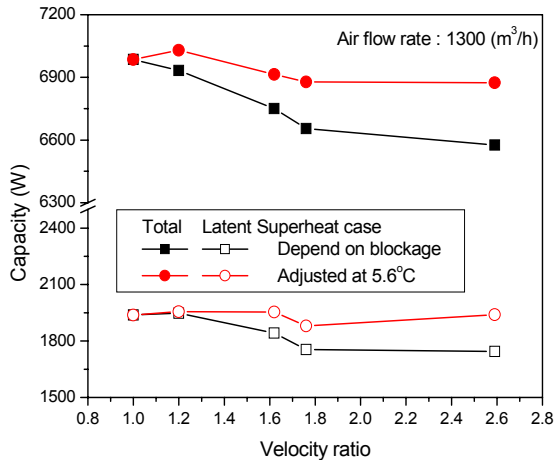


Figure 5: Capacity for different air velocity ratios at constant volumetric air flow rate

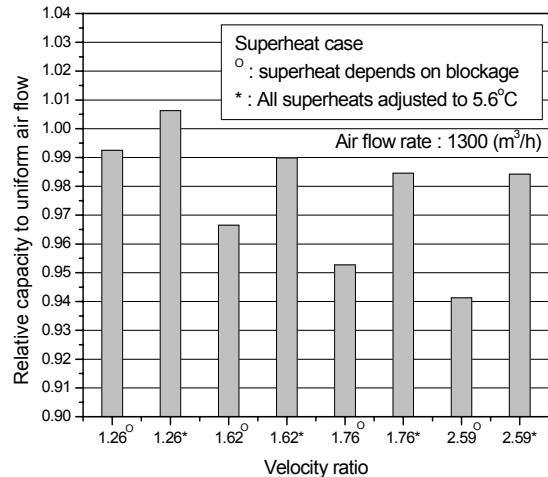


Figure 6: Capacity for different air velocity ratios referenced to the baseline capacity at constant volumetric air flow rate

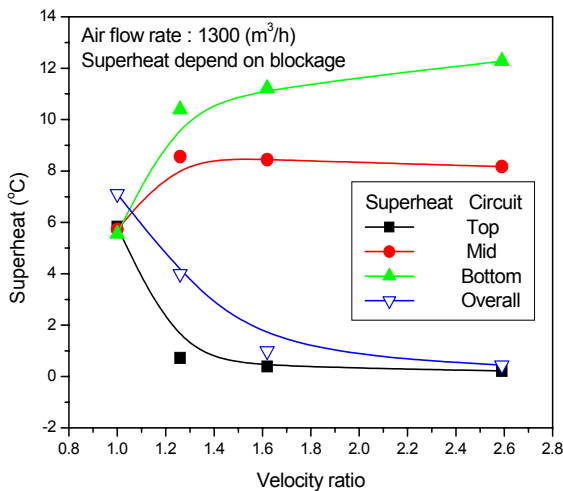


Figure 7: Individual circuit and overall superheats for different air velocity ratios at constant volumetric air flow rate

Figure 7 shows overall superheat and individual circuit superheats that were caused by different air velocity ratios via different mesh obstructions. Since the volumetric flow rate of air was the same for all tests, the blockage of the upper half of the coil was simply displacing the air flow from the upper to the lower part of the coil. Consequently, increasing the blockage on the upper half of the coil resulted in reduced superheat and flooding at the top circuit, while the superheats at the middle and bottom circuits increased substantially. In the case of the 1:1.20 velocity profile, the difference in superheat between top circuit and bottom circuit increased by 10.4 °C. For the 1:2.6 velocity ratio, superheat difference increased to 12.2 °C. The resulting overall superheat decreased also. For the largest blockage

corresponding to the 1:2.6 velocity ratio, the evaporator exit sight glass showed two-phase refrigerant.

It should be noted that these tests were conducted at a constant evaporator exit pressure contrary to a real system which will respond to a loss of air flow with a drop in the evaporator pressure. Hence, the disparity between different circuit superheats in a real system will be greater than that reported here because there will be a larger temperature difference between the inlet air and refrigerant saturation temperature.

2.2.2 Reduced Air Flow Rate: Tests with a reduced air flow correspond to an installation scenario where the air flow rate is reduced below the nominal value due to obstruction on the air side that was not rectified by an increase in fan speed. The obstruction may be due to duct configuration, clogged filters, bent fins, etc. Figure 8 shows absolute values of capacity for different velocity ratios, and Figure 9 the capacities referenced to the baseline capacity and the nominal volumetric air flow. As for the tests with a constant air flow rate presented in section 2.2.1, different air velocity ratios were obtained by adding different levels of air obstruction to the upper half of the evaporator; however, the volumetric flow rate was allowed to change with the obstruction. Figures 8 and 9 show a trend similar to capacity variation with constant air flow rate (Figures 5 and 6), but the slope of capacity with velocity ratio is more negative. For the velocity ratio of 1.76, the drop in capacity is as much as 8.7 % while it was 4.7 % for the case with a constant air flow rate. Controlling refrigerant distribution between different circuits to maintain individual superheats at 5.6 °C increased the capacity by up to 4 % for the 1.76 air velocity ratio.

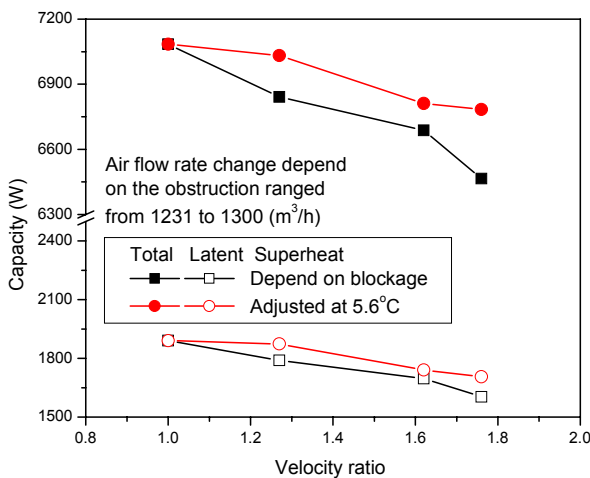


Figure 8: Capacity for different air velocity ratios at volumetric air flow rates reduced by obstruction

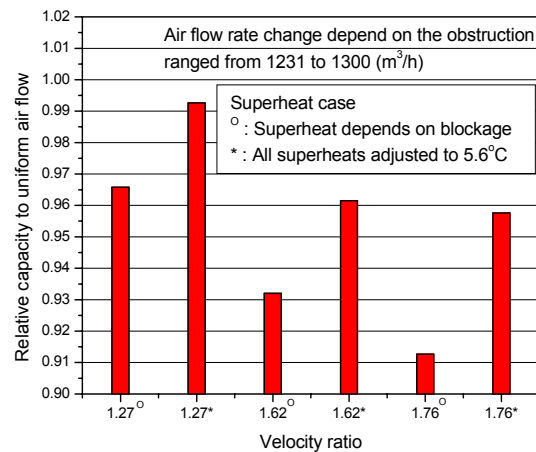


Figure 9: Capacity for different air velocity ratios with air flow rates reduced by obstruction, referenced to the baseline capacity

Refrigerant superheat in a given circuit is affected by the refrigerant mass flow rate and the air flow rate over the coil area associated with that circuit. For a given air distribution there is one refrigerant flow rate that results in a desired superheat at the individual circuit exit. When circuits are not well balanced, the target overall superheat is a result of mixing a highly superheated refrigerant and two-phase refrigerant leaving different circuits. This causes significant degradation in evaporator capacity because the circuit with superheated refrigerant transfers less heat.

Figure 10 shows the relative coil air pressure drop with respect to velocity ratio changes due to blockage of the upper half of the evaporator. In case of the 1:1.27 velocity ratio, the obstruction would have increased fan power by more than 14 %, based on the fan law and assuming an ideal fan. For 1:1.76 velocity ratio, the fan power would have increased by at least 34 % relative to the uniform air flow case.

Figure 10 shows that the air pressure drop across the coil for the 5.6 °C superheat tests are consistently higher than those for the tests with uncontrolled superheat. This is likely related to a higher latent capacity for the 5.6 °C superheat tests, shown in Figure 8. It is safe to speculate that the higher latent capacity resulted in a thicker layer of condensate on the coil, which offered more air flow resistance.

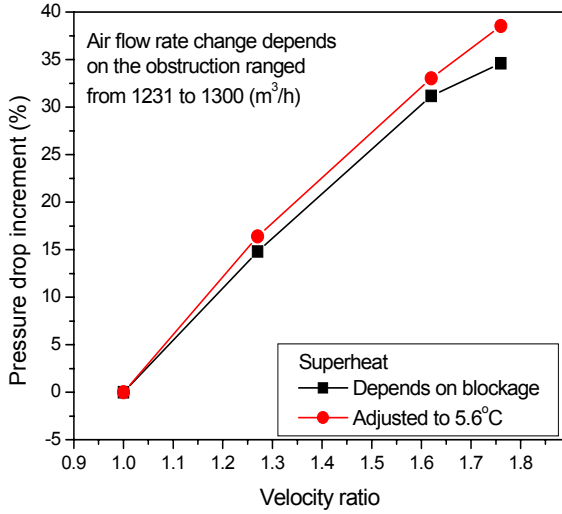


Figure 10: Evaporator air pressure drop for different velocity ratios at volumetric air flow rates reduced by obstruction

2.2.3 Constant versus reduced air flow rate results: As capacity loss increased with the air velocity ratio (blockage), so increased the opportunity to recover the lost capacity by controlling refrigerant distribution. This opportunity exist whether air flow rate was constant or not, but is somewhat higher for the reduced volumetric flow rate system installation scenario. Figure 11 presents capacity improvement due to control of refrigerant superheat, referenced to the degraded capacity. For a scenario with a reduced volumetric flow rate, the recovery in capacity with superheat adjusted to the original 5.6 °C is 2.8 % at the 1:1.27 velocity ratio and 4.9 % at the 1:1.76 velocity ratio.

superheated refrigerant was approaching the inlet air temperature of 26.7 °C (refrigerant saturation temperature was of 7.2 °C, and the superheat was higher than 10 °C). This approach to the air temperature was more rapid for constant volumetric flow rate tests than for reduced volumetric air flow tests.

Figure 12 presents the superheat standard deviation between all of the circuits with respect to the evaporator exit superheat. The superheat standard deviation appears to be approaching a plateau near the air velocity ratio of 2. This is caused by the fact that

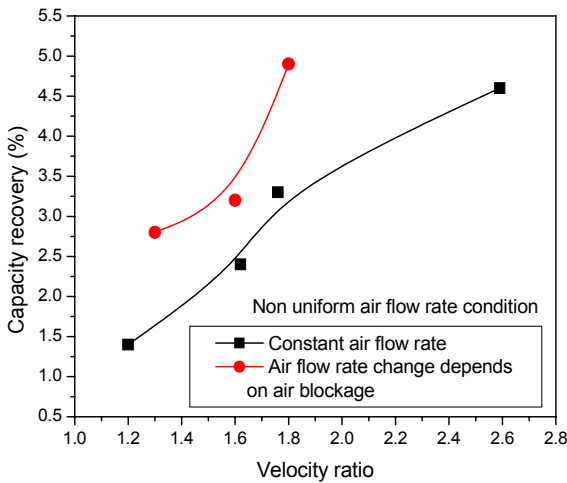


Figure 11: Capacity recovery by superheat adjustment, referenced to the degraded capacity, as a function of velocity ratio

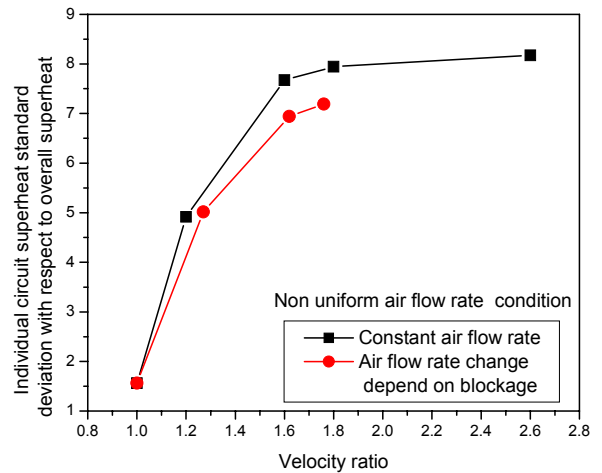


Figure 12 : Circuit superheat standard deviation with respect to overall superheat as a function of velocity ratio

CONCLUSIONS

This experimental investigation was implemented to determine the capacity degradation due to non-uniform refrigerant and airflow distributions, and to assess the potential to recover the lost capacity via controlling refrigerant distribution between individual circuits. During the tests, individual expansion valves were used on each circuit to control individual exit superheats. The tests were performed on a three-circuit, three-depth-row, finned-tube evaporator.

The study showed that capacity degradation due to refrigerant maldistribution can be as much as 30 %, even when the overall evaporator superheat is kept at the target 5.6 °C. Experimental data indicate that part of this capacity degradation was caused by the internal heat transfer within the evaporator assembly.

Two maldistributed air flow scenarios were studied: one, assuming constant volumetric flow of air, and the other, assuming the volumetric flow rate to decrease with the air flow obstruction. For the coil and air maldistributions studied, the maximum capacity degradation was found to be 8.7 %. A 4.0% capacity recovery was obtained by controlling refrigerant distribution to obtain the target 5.6 °C at each circuit exit.

It should be noted that all tests were conducted at a constant evaporator exit pressure while a real system responds with a drop in the evaporator pressure to any reduction of evaporator capacity. Hence, the disparity between different circuit superheats in a real system will be greater than that reported here because there will be a larger temperature difference between the inlet air and refrigerant saturation temperature.

ACKNOWLEDGMENT

This work was sponsored by the Air-Conditioning and Refrigeration Technology Institute (ARTI) under ARTI 21-CR Program Contract Number 605-20050, managed by E. Jones. We acknowledge the comments and support by members of the ARTI 21-CR Equipment Energy Efficiency Subcommittee.

REFERENCES

- ANSI/AMCA Standard 210, 1985, Laboratory Methods of Testing Fans for Rating. American Society of Heating, Refrigerating and Air-Conditioning Engineers., Atlanta.
- ANSI/ASHRAE Standard 37, 1988., Methods of Testing for Rating Unitary Air Conditioning and Heat Pump Equipment, American Society of Heating, Refrigerating and Air-Conditioning Engineers., Atlanta.
- Bergles, A.E., Collier, J.G., Delhaye, J.M., Hewitt, G.F., and Mayinger, F., 1981, Two-Phase Flow and Heat Transfer in the Power and Process Industries, Hemisphere Publishing Corp., New York, p. 146-147.
- Chwalowski, M., Didion, D. A., and Domanski, P. A., 1989, Verification of Evaporator Computer Models and Analysis of Performance of an Evaporator Coil, ASHRAE Trans., Vol. 95, no. 1.
- Domanski, P.A. and McLinden, M.O., 1992, A Simplified Cycle Simulation Model for the Performance Rating of Refrigerants and Refrigerant Mixtures, Int. Journal of Refrigeration, Vol. 15, no 2: p. 81-88.
- Kirby, E. S., C. W. Bullard, and W. E. Dunn, 1998, Effect of Airflow Nonuniformity on Evaporator Performance, Transactions of the American Society of Heating, Refrigeration, and Air Conditioning Engineers, Vol.104, no. 2: p. 755-762.
- Lee, J., Domanski, P. A., 1997, Impact of Air and Refrigerant Maldistributions on the Performance of Finned-Tube Evaporators with R22 and R407C, Report DOE/CE/23810-81 for ARI, National Institute of Standards and Technology, Gaithersburg, MD.
- Liang S.Y., Wong T.N., Nathan G.K., 2001, Numerical and experimental studies of refrigerant circuitry of evaporator coils, International Journal of Refrigeration, Vol. 24: p.823-833.
- Payne, W. Vance and Domanski, Piotr A., 2003, Potential benefits of smart refrigerant distributors, ARTI-21CR/605-200-50-01, Air-Conditioning and Refrigeration Technology Institute, 4100 North Fairfax Drive, Suite 200, Arlington, Virginia USA, 22203.